

Quark Imaging in the Proton Via Quantum Phase-Space Distributions

A.V. Belitsky,^{*} Xiangdong Ji,[†] and Feng Yuan[‡]

*Department of Physics,
University of Maryland
College Park, Maryland 20742*

*Institute for Nuclear Theory,
University of Washington
Box 351550, Seattle, WA, 98195*

(Dated: October 23, 2018)

Abstract

We develop the concept of quantum phase-space (Wigner) distributions for quarks and gluons in the proton. To appreciate their physical content, we analyze the constraints from special relativity on the interpretation of elastic form factors, and examine the physics of the Feynman parton distributions in the proton's rest frame. We relate the quark Wigner functions to the transverse-momentum dependent parton distributions and generalized parton distributions, emphasizing the physical role of the skewness parameter. We show that the Wigner functions allow to visualize quantum quarks and gluons using the language of the classical phase space. We present two examples of the quark Wigner distributions and point out some model-independent features.

^{*}Electronic address: belitsky@physics.umd.edu

[†]Electronic address: xji@physics.umd.edu

[‡]Electronic address: fyuan@physics.umd.edu

I. INTRODUCTION

In exploring the microscopic structure of matter, there are two frequently-used approaches. First, the spatial distribution of matter (or charge) in a system can be probed through elastic scattering of electrons, or photons, or neutrons, etc. The physical quantity that one measures is the elastic form (structure) factors which depend on three-momentum transfer to the system. The Fourier transformation of the form factors provides direct information on the spatial distributions. The well-known examples include the study of charge distribution in an atom and the atomic structure of a crystal. The second approach is designed to measure the population of the constituents as a function of momentum, or the momentum distribution, through knock-out scattering. Here the well-known examples include the nucleon distributions in nuclei measured through quasi-elastic electron scattering, and the distribution of atoms in a quantum liquid probed through neutron scattering. The scattering cross section sometimes depends on the reaction dynamics which must be understood before the momentum distribution can be extracted.

Both approaches are complementary, but bear similar drawbacks. The form factor measurements do not yield any information about the underlying dynamics of the system such as the speed of the constituents, whereas the momentum distribution does not give any information on the spatial location of the constituents. More complete information about the microscopic structure lies in the correlation between the momentum and coordinate spaces, i.e., to know where a particle is located and, at the same time, with what velocity it travels. This information is certainly attainable for a classical system for which one can define and study the phase-space distribution of the constituents. For a quantum mechanical particle, however, the notion of a phase-space distribution seems less useful because of the uncertainty principle. Nonetheless, the first phase-space distribution in quantum mechanics was introduced by Wigner in 1932 [1], and many similar distributions have been studied thereafter. These distributions have been used for various purposes in very diverse areas such heavy-ion collisions, quantum molecular dynamics, signal analysis, quantum information, optics, image processing, non-linear dynamics, etc.[2] In certain cases, the Wigner distributions can even be measured directly in experiments [3, 4, 5], providing much information about the dynamics of a system.

The main interest of this paper is about the internal structure of the proton (or neutron), for which the underlying fundamental theory is quantum chromodynamics (QCD). With some changes to accommodate the relativistic nature of the problem, both experimental approaches alluded to above have been successfully used to unravel its quark and gluon structure: The elastic form factors of the proton have been measured since the 1950s and, at low-momentum transfer (\leq nucleon mass M_N) where the nucleon recoil effects are small, the three-dimensional (3D) Fourier transformation of these form factors can be interpreted as spatial charge and current distributions of quarks [6]. Feynman parton distributions, measurable in high-energy inelastic scattering such as deep-inelastic scattering (DIS) and Drell-Yan process, have a simple interpretation as the momentum distributions of the quarks and gluons in the infinite momentum frame (IMF) [7]. However, the notion of correlated position and momentum distributions of quarks and gluons has not been systematically investigated in the field, although it is clear that the physics of a phase-space distribution must be very rich.

In this paper, we explore to what extent one can construct physically-interesting and experimentally-measurable phase-space distributions in QCD, and what information it con-

tains about the QCD parton dynamics. [A brief account of some of the results can be found in Ref. [8], see also [9].] To facilitate the construction, we examine the uncertainty in the traditional interpretation of electromagnetic form factors due to relativity, and analyze the physical content of the Feynman parton distributions in the rest frame of the proton. We then introduce the phase-space Wigner distributions for the quarks and gluons in the proton, which contain most general one-body information of partons, corresponding to the full one-body density matrix in technical terms. After integrating over the spatial coordinates, one recovers the familiar transverse-momentum dependent parton distributions [10]. On the other hand, some reduced version of the distributions is related, through a specific Fourier transformation, to the generalized parton distributions (GPDs) which have been studied extensively in the literature in recent years [11, 12, 13, 14, 15, 16, 17]. Roughly speaking, a GPD is a one-body matrix element which combines the kinematics of both elastic form factors and Feynman parton distributions, and is measurable in hard exclusive processes. Therefore, the notion of phase-space distribution provides a new 3D interpretation of the GPDs in the rest frame of the proton. There are other interpretations of the GPD in the literature which are made in IMF and impact parameter space [18, 19, 20, 21, 22].

The presentation of the paper is as follows. In Section II, we examine the constraints on the physical interpretation of the form factors and parton distributions from relativistic effects, anticipating their extension to a full phase-space distribution. In Section III, we first briefly summarize the main features of a quantum mechanical Wigner distribution, then introduce the quantum phase-space distributions for the quarks and gluons in a rest-frame proton. In Section IV, we exhibit the spatial 3D images of quarks generated from slicing the quantum phase-space (Wigner) distributions at different Feynman momentum and comment on their general features. Section V contains the summary and conclusion.

II. RELATIVITY CONSTRAINT ON INTERPRETATION OF FORM FACTORS AND PARTON DISTRIBUTIONS

In the literature, the quantum phase-space distributions have been mostly applied to non-relativistic systems. For the proton, however, relativity is essential. In measuring the elastic form factors of the proton, the momentum transfer to the system can easily exceed the rest mass, resulting a large recoil and Lorentz contraction. The quarks and gluons inside the proton follow relativistic dynamics. Moreover, when a quark is struck in a DIS experiment, it travels along the light-cone: the trajectory of an extreme-relativistic particle. Therefore, to develop a phase-space distribution of the proton, we must examine to what extent the notion actually makes sense for relativistic systems.

In the first subsection, we examine the textbook interpretation of the electromagnetic form factors of the proton, reminding the reader that there are intrinsic ambiguities in the interpretation. We emphasize, however, that different ways of the interpreting the form factors can be regarded as different choices of schemes. When used consistently, one scheme is in principle as good as any other. The degree of scheme dependence depends on $1/(MR)$, where M is the mass and R is some kind of radius, which is $1/4$ for the proton.

In the second subsection, we consider the Feynman parton distributions, most-commonly interpreted as the momentum densities in IMF. Since the notion of a phase-space distribution is meant for a proton in its *rest frame*, and since the distribution should be reduced to the Feynman distribution after integrating out the spatial coordinates, we are compelled to examine the physics of latter in the static system of coordinates. In particular, we need to

understand the meaning of Feynman momentum x in that context. This can be achieved by introducing the so-called *spectral function*—the correlated momentum and energy distribution of the constituents—familiar in non-relativistic many-body physics. In the process, we find that the separation between particle and antiparticle, familiar in the IMF, disappears: One can only keep track of the creation and annihilation of fermion quantum numbers, such as the electric charge.

A. The Proton Form Factors and Scheme-Dependent Charge Distributions

The electromagnetic form factors are among the first measured and mostly studied observables of the nucleon. They are defined as the matrix elements of the electromagnetic current between the nucleon states of different four-momenta. Because the nucleon is a spin one-half particle, the matrix element defines two form factors,

$$\langle p_2 | j_\mu(0) | p_1 \rangle = \bar{U}(p_2) \left\{ F_1(q^2) \gamma_\mu + F_2(q^2) \frac{i\sigma_{\mu\nu} q_\nu}{2M_N} \right\} U(p_1), \quad (1)$$

where F_1 and F_2 are the well-known Dirac and Pauli form factors, respectively, depending on the momentum transfer $q = p_2 - p_1$, and $U(p)$ is nucleon spinor normalized as $\bar{U}(p)U(p) = 2M_N$.

Since the beginning, it has been known that the physical interpretation of the nucleon form factors is complicated by relativistic effects [23]. Consider a system of size R and mass M . In relativistic quantum theory, the system cannot be localized to a precision better than its Compton wavelength $1/M$. Any attempt to do this with an external potential will result in creation of particle-antiparticle pairs. As a consequence, the static size of the system cannot be defined to a precision better than $1/M$. If $R \gg 1/M$, which is the case for all non-relativistic systems, the above is not a significant constraint. One can probe the internal structure of the system with a wavelength $(1/|\vec{q}|)$ comparable to or even much smaller than R , but still large enough compared to $1/M$ so that the probe does not induce an appreciable recoil. A familiar example is the hydrogen atom for which $RM_H \sim M_H/(m_e\alpha_{\text{em}}) \sim 10^5$, and the form factor can be measured through electron scattering with momentum transfer $|\vec{q}| \ll M_H$.

When the probing wavelength is comparable to $1/M$, the form factors are no longer determined by the internal structure alone. They contain also the dynamical effects of Lorentz boosts because the initial and final protons have different momenta. In relativistic quantum theory, the boost operators involve nontrivial dynamical effects which result in the nucleon wave function being different in different frame (in the usual instant form of quantization). Therefore in the region $|\vec{q}| \sim M$, the physical interpretation of the form factors is complicated because of the entanglement of the internal and the center-of-mass motions in relativistic dynamics. In the limit $|\vec{q}| \gg M$, the former factors depend almost entirely on the physical mechanism producing the overall change of the proton momentum. The structural effect involved is a very small part of the nucleon wave function (usually the minimal Fock component only).

For the nucleon, $M_N R_N \sim 4$. Although much less certain than in the case of the hydrogen atom, it seems still sensible to have a rest-frame picture in terms of the electromagnetic form factors, so long as one keeps in mind that equally justified definitions of the nucleon sizes can differ by $\sim 1/M_N(R_N M_N)$. For example, the traditional definition of the proton charge radius in terms of the slope of the Sachs form factor $G_E(q^2)$ is 0.86 fm. On the other hand,

if one uses the slope of the Dirac form factor F_1 to define the charge radius, one gets 0.79 fm, about 10% smaller. The form factors at $|\vec{q}| \geq M_N \sim 1$ GeV cannot be interpreted as information about the internal structure alone.

To further clarify the uncertainty involved in the interpretation of the electromagnetic form factors, let us review the textbook explanation offered originally by Sachs [6].

To establish the notion of a static (charge) distribution, one needs to create a wave-packet representing a proton localized at \vec{R}

$$|\vec{R}\rangle = \int \frac{d^3\vec{p}}{(2\pi)^3} e^{i\vec{p}\cdot\vec{R}} \Psi(\vec{p}) |\vec{p}\rangle, \quad (2)$$

where the plane-wave state $|\vec{p}\rangle$ is normalized in a relativistic-covariant manner $\langle\vec{p}_2|\vec{p}_1\rangle = 2E_{\vec{p}_1}(2\pi)^3\delta^{(3)}(\vec{p}_1 - \vec{p}_2)$, and $\Psi(\vec{p})$ is the momentum space profile normalized as $2\int d^3\vec{p} E_{\vec{p}} |\Psi(\vec{p})|^2 = (2\pi)^3$. The wave-packet is not an eigenstate of the free Hamiltonian. Therefore, as time progresses, the wave packet will spread. The characteristic spreading time is proportional to $\langle M_N/\vec{p}^2 \rangle$ which is long for a non-relativistic system. But for a relativistic particle, the spread could happen much faster compared to the characteristic time-scale of a weakly-interacting probe.

Having localized the wave-packet at $\vec{R} = 0$, we can calculate, for example, the charge distribution in the wave-packet

$$\rho(\vec{r}) = \langle \vec{R} = 0 | j_0(\vec{r}) | \vec{R} = 0 \rangle, \quad (3)$$

where \vec{r} measures the relative distance to the center $\vec{R} = 0$. Taking its Fourier transform, one gets

$$\begin{aligned} F(\vec{q}) &\equiv \int d^3\vec{r} e^{i\vec{q}\cdot\vec{r}} \rho(\vec{r}) \\ &= \int \frac{d^3\vec{p}}{(2\pi)^3} \Psi^*(\vec{p} + \vec{q}/2) \Psi(\vec{p} - \vec{q}/2) \langle \vec{p} + \vec{q}/2 | j_0(0) | \vec{p} - \vec{q}/2 \rangle, \end{aligned} \quad (4)$$

where we have changed the momentum integration variables, with \vec{p} representing the average momentum of the initial and final protons. It is important to point out that the resolution momentum \vec{q} is now linked to the difference in the initial and final state momenta. In non-relativistic quantum systems, because of the large masses, the momentum transfer causes little change in velocity, and hence the initial and final states have practically the same intrinsic wave functions. In relativistic systems, this is the origin of the difficulty in interpreting the form-factor: we do not have a matrix element involving the same intrinsic proton state.

To remove the effects of the wave packet, the necessary condition on $\Psi(\vec{p})$ is that the coordinate-space size of the wave-packet must be much smaller than the system size $|\delta\vec{r}| \ll R_N$. Furthermore, the probing wave length, or resolution scale, must also be large compared with the size of the wave-packet $\delta\vec{r} \sim 1/\vec{p} \ll 1/\vec{q}$. Then one can ignore \vec{q} -dependence in Ψ , so that $\Psi(\vec{p} \pm \frac{1}{2}\vec{q}) \approx \Psi(\vec{p})$

$$F(\vec{q}) = \int \frac{d^3\vec{p}}{(2\pi)^3} |\Psi(\vec{p})|^2 \langle \vec{p} + \vec{q}/2 | j_0(0) | \vec{p} - \vec{q}/2 \rangle. \quad (5)$$

On the other hand, to be insensitive to the anti-particle degrees of freedom, the size of the wave packet must be larger than the proton Compton wave length $|\delta\vec{r}| \gg 1/M_N$. In the

momentum space this corresponds to restrictions on momenta allowed in the wave packet $|\vec{p}| \ll M_N$. Therefore the combined constraint on the wave packet profile is $1/R_N \ll |\vec{q}| \ll |\vec{p}| \ll M_N$. The extreme limit of the last inequality yields a wave packet with a zero-momentum nucleon

$$|\Psi(\vec{p})|^2 = \frac{(2\pi)^3}{2M_N} \delta^{(3)}(\vec{p}), \quad (6)$$

which gives

$$2M_N F(\vec{q}) = \langle \vec{q}/2 | j_0(0) | -\vec{q}/2 \rangle. \quad (7)$$

This is the matrix element of the charge density in the Breit frame, and is $2M_N G_E(t) w_2^* w_1$ where

$$G_E(t) = F_1(t) + \frac{t}{4M_N^2} F_2(t) \quad (8)$$

is the Sachs electric form factor ($t = -\vec{q}^2$) and the Weyl spinors involved are normalized conventionally by $w^* w = 1$. Hence, we arrive at the textbook interpretation of G_E as a Fourier transformation of the proton charge distribution.

Likewise, the Sachs magnetic form factor $G_M(t) = F_1(t) + F_2(t)$ is obtained from the Breit frame matrix element of the electric current

$$\langle \vec{q}/2 | \vec{j}(0) | -\vec{q}/2 \rangle = 2i[\vec{s} \times \vec{q}] G_M(t), \quad (9)$$

where the three-vector of spin is $\vec{s} = w_2^* \frac{1}{2} \vec{\sigma} w_1$.

It must be pointed out that the charge and magnetization distributions thus defined contains the Lorentz contraction effects along the photon direction \vec{q} when $\vec{q}^2 \gg 4M_N^2$, which make the proton look like a pancake. Various prescriptions exist in the literature which have been proposed to remove the relativity effects and extract the “intrinsic” charge/magnetization distributions from the experimental data [24, 25, 26]. However, it is difficult to accomplish it in a model-independent way.

Since relativity makes the interpretation of the electromagnetic form factors non-unique, the best one can do is to choose one particular interpretation and work consistently. For example, when extracting the proton charge radius from the Lamb shift measurements, one shall use the same definition as from the electric form factor. The most frequently-used definition is that of Sachs, but other schemes are equally good and the scheme dependence disappears in the limit $MR \rightarrow \infty$. This is very much like the renormalization scheme dependence of parton densities due to radiative corrections at finite strong coupling constant α_s : Although the $\overline{\text{MS}}$ scheme is the most popular in the literature, one can use the parton densities in any other scheme to correlate physical observables. In this paper, we adopt the Sachs interpretation of the form factors.

Relativistic corrections and Lorentz contraction effects in the transverse dimensions are found to disappear in an IMF [19]. There the proton has an infinitely large effective mass, and hence for physics in the transverse dimensions, we are back to the non-relativistic case. In particular, one can localize the proton in the transverse coordinate space with no recoil corrections. The Dirac form factor F_1 is found to be related to the charge distribution in transverse plane, with information along the z -axis integrated. The price one pays for eliminating the relativistic effects is the loss of a spatial dimension.

B. Parton Distributions As Seen in the Rest Frame of the Proton

Parton distributions were introduced by Feynman to describe deep-inelastic scattering [7]. They have the simplest interpretation in the IMF as the densities of partons in the longitudinal momentum x . In QCD, the quark distribution is defined through the following matrix element,

$$q(x) = \frac{1}{2p^+} \int \frac{d\lambda}{2\pi} e^{i\lambda x} \langle p | \bar{\Psi}(0) \gamma^+ \Psi(\lambda n) | p \rangle, \quad (10)$$

where we have used the standard light-cone notation $p^\pm = (p^0 \pm p^3)/\sqrt{2}$, and n^μ is a vector along the direction of $(1, 0, 0, -1)$ and $n \cdot p = 1$. Ψ is a quark field with an associated gauge link extending from the position of the quark to infinity along the light cone, and hence is gauge-invariant in non-singular gauges. The renormalization scale dependence is implicit. In light-cone quantization [27], it is easy to get

$$\begin{aligned} q(x)|_{x>0} &= \frac{1}{2x} \sum_{\lambda=\uparrow\downarrow} \int \frac{d^2 \vec{k}_\perp}{(2\pi)^3} \frac{\langle p | b_\lambda^\dagger(k^+, \vec{k}_\perp) b_\lambda(k^+, \vec{k}_\perp) | p \rangle}{\langle p | p \rangle}, \\ q(x)|_{x<0} &= \frac{-1}{2x} \sum_{\lambda=\uparrow\downarrow} \int \frac{d^2 \vec{k}_\perp}{(2\pi)^3} \frac{\langle p | d_\lambda^\dagger(k^+, \vec{k}_\perp) d_\lambda(k^+, \vec{k}_\perp) | p \rangle}{\langle p | p \rangle}, \end{aligned} \quad (11)$$

where b^\dagger and d^\dagger are creation operators of a quark and an anti-quark, respectively, with longitudinal momentum $k^+ \equiv xp^+$ and transverse momentum \vec{k}_\perp . The interpretation as parton densities is then obvious.

To construct the quantum phase-space distributions for the quarks, we need an interpretation of the Feynman densities in the rest frame. This is because the IMF involves a Lorentz boost along the z -direction which destroys the rotational symmetry of the 3D space. However, if one works in the rest frame of the proton, the two quark fields in Eq. (10) are not at the same time. If one Fourier-expands one of the fields in terms of quark creation and annihilation operators, the other must be determined from Heisenberg equation of motion. The result is that the bi-linear quark operator takes a very complicated expression in terms of the creation and annihilation operators in the equal-time quantization.

The physics of the Feynman quark distribution in the rest frame is made more clear through the notion of the *spectral function*

$$S(k) = \frac{1}{2p^+} \int d^4 \xi e^{ik \cdot \xi} \langle p | \bar{\Psi}(0) \gamma^+ \Psi(\xi) | p \rangle. \quad (12)$$

which is the dispersive part of the single-quark Green's function in the proton. The physical meaning of $S(k)$ can be seen from its spectral representation,

$$\begin{aligned} S(k) &= \sum_n (2\pi)^4 \delta^{(4)}(p - k - p_n) \langle p | \bar{\Psi}_k | n \rangle \gamma^+ \langle n | \Psi(0) | p \rangle / 2p^+ \\ &\sim \sum_n (2\pi)^4 \delta^{(4)}(p - k - p_n) |\langle n | \Psi_{k+} | p \rangle|^2 \end{aligned} \quad (13)$$

where Ψ_k is a Fourier transformation of $\Psi(\xi)$: It is the probability of annihilating a quark (or creating an antiquark) of *four*-momentum k (three-momentum \vec{k} and the off-shell energy $E = k^0$) in the nucleon, leading to an “on-shell” state of energy-momentum $p_n = p - k$. The

quark here is off-shell because if p_n and p are both “on-shell”, $k^2 \neq m_q^2$ in general. [That the partons are off-shell are in fact also true in the IMF calculations.] Of course, in QCD $|n\rangle$ is not in the Hilbert space, but the spectral function itself is still a meaningful quantity.

Since the quarks are ultra-relativistic, Ψ_k contains both quark and antiquark Fock operators. One cannot in general separate quark and anti-quark contributions, unlike in the non-relativistic systems in which only the particle or antiparticle contribute. In fact, if one expands the above expression, one finds pair creations and annihilation terms. However, this is also true for the charge density discussed in the previous subsection. Therefore we can speak of $S(k)$ as a distribution of vector charges and currents, but not a particle density. In nuclear physics where the non-relativistic dynamics dominates, the nucleon spectral function in the nucleus is positive definite and can be regarded as a particle density. The nuclear spectral function is directly measurable through pick-up and knock-out experiments, in which E and \vec{k} are called the missing energy and missing momentum, respectively (see for example [28]).

It is now easy to see that in the rest frame of the proton, the Feynman quark distribution is

$$q(x) = \sqrt{2} \int \frac{d^4 k}{(2\pi)^4} \delta(k^0 + k^z - xM_N) S(k) . \quad (14)$$

The x variable is simply a special combination of the off-shell energy k^0 and momentum k^z . The parton distribution is the spectral function of quarks projected along a special direction in the four-dimensional energy-momentum space. The quarks with different k^0 and k^z can have the same x , and moreover, the both $x > 0$ and $x < 0$ distributions contain contributions from quarks and anti-quarks.

To summarize, in the proton rest frame, the quarks are naturally off-shell, and hence have a distribution in the four-dimensional energy-momentum space. The Feynman distribution comes from a reduction of the full distribution along a special direction.

III. QUANTUM PHASE-SPACE (WIGNER) DISTRIBUTIONS

In classical physics, a state of a particle is specified by its position \vec{r} and momentum \vec{p} . In a gas of classical particles, the single-particle properties are described by a phase-space distribution $f(\vec{r}, \vec{p})$ representing the density of particles at a phase-space point (\vec{r}, \vec{p}) . Time evolution of the distribution is governed by the Boltzmann equation, or Liouville equation if the particles are not interacting.

In quantum mechanics, position and momentum operators do not commute and hence, in principle, one cannot talk about a joint momentum and position distribution of particles. Indeed the quantum mechanical wave functions depend on either spatial coordinates or momentum, but never both. Nonetheless, Wigner introduced the first quantum phase-space distribution just a few years after quantum mechanics was formulated [1]. It is not positive definite and hence cannot be regarded as a probability distribution. However, it reduces to the positive-definite classical phase-space distribution in $\hbar \rightarrow 0$ limit. The sign oscillation in the phase-space is necessary to reproduce quantum interference. The Wigner distribution contains the complete single-particle information about a quantum system (equivalent to the full single-particle density matrix), and can be used to calculate any single-particle observable through classical-type phase-space averages.

In this section, we first remind the reader some basic features of the quantum phase-space (Wigner) functions. We then generalize the concept to the relativistic quarks and gluons in

the proton. With the preparation in Section II, the construction is straightforward. However, the most general phase-space distribution we define is not measurable at present, and hence we proceed to make reductions by integrating out some dependent variables. After integrating out the spatial coordinates, we recover the transverse-momentum dependent parton distributions[10]. Upon integrating over the parton transverse momentum, we have the reduced Wigner distributions depending on 3-space coordinates and Feynman momentum x , which are related to the GPDs by a simple Fourier transformation. Therefore, the reduced quantum phase-space distributions are physical observables.

A. General Aspects of Wigner Distributions

There is a vast literature on the quantum phase-space distributions, and the Wigner distributions in particular. In this subsection, we would like to summarize some of the salient features.

Suppose we have a one-dimensional quantum mechanical system with wave function $\psi(x)$, the Wigner distribution is defined as

$$W(x, p) = \int d\eta e^{ip\eta} \psi^*(x - \eta/2) \psi(x + \eta/2) , \quad (15)$$

where we have set $\hbar = 1$. When integrating out the coordinate x , one gets the momentum density $|\psi(p)|^2$, which is positive definite. When integrating out p , the positive-definite coordinate space density $|\psi(x)|^2$ follows. For arbitrary p and x , the Wigner distribution is not positive definite and does not have a probability interpretation. Nonetheless, for calculating the physical observables, one can just take averages over the phase-space as if it is a classical distribution

$$\langle \hat{O}(x, p) \rangle = \int dx dp W(x, p) O(x, p) \quad (16)$$

where the operators are ordered according to the Weyl association rule. For a single-particle system, the Wigner distribution contains everything there is in the quantum wave function. For a many-body system, the Wigner distribution can be used to calculate the averages of all one-body operators. Sign changes in the phase-space are a hint that it carries non-trivial quantum phase information.

In the classical limit, the Wigner distribution is expected to become classical phase-space distribution. For systems which are statistical ensembles, the limit $\hbar \rightarrow 0$ is often well-behaved. For example, for an ensemble of harmonic oscillators at finite temperature, the Wigner distribution becomes the classical Boltzmann distribution as $\hbar \rightarrow 0$, see, e.g., [29]. The Wigner distribution for the n th excited state of the one-dimensional harmonic oscillator of energy $E_n = \hbar\omega \left(n + \frac{1}{2}\right)$ is [30]

$$W_n(p, x) = \frac{(-1)^n}{\pi \hbar} e^{-2H/(\hbar\omega)} L_n \left(\frac{4H}{\hbar\omega} \right) , \quad (17)$$

where H stands for the hamiltonian $H(p, x) = p^2/(2m) + m\omega^2 x^2/2$ and L_n is the n th Laguerre polynomial. In the quasi-classical limit—vanishing Planck constant and large quantum numbers—the oscillator Wigner distribution turns into the generalized distribution resided on the classical trajectories $E_\infty = \text{fixed}$,

$$\lim_{\hbar \rightarrow 0, n \rightarrow \infty} W_n(p, x) \sim \delta(H(p, x) - E_\infty) . \quad (18)$$

Phase-space averaging with this kernel is equivalent to calculating observables using classical equations of motion. This can be easily understood from the semi-classical form of the wave function

$$\psi(x) = C(x)e^{iS(x)/\hbar} . \quad (19)$$

Substituting this into Eq. (15) and expanding S to the first order in \hbar , one gets the quasi-classical Wigner distribution

$$W(p, x) = |C|^2 \delta \left(p - \frac{\partial S(x)}{\partial x} \right) , \quad (20)$$

where the argument of the delta-function describes a family of classical paths.

The quantum-mechanical Wigner distribution is measurable. The actual measurement has been performed for a simplest quantum system—the quantum state of a light mode (a pulse of laser light of given frequency)—employing ideas of Vogel and Risken [3]. It was extracted via the method of homodyne tomography [4] by measurement of a marginal observable and subsequent reconstruction by the inverse Radon transformation. Recently this Wigner distribution has been measured directly by means of the photon counting techniques based on a Mach-Zender interferometric scheme [5].

Other versions of the phase-space distributions are possible. They are all members of the so-called Cohen class [31], with Husimi and Kirkwood distributions [32] being its well-known representatives. The Husimi distribution is a smeared version of the Wigner distribution defined by projection of the wave function on the coherent state (Gaussian wave packet)

$$H(\bar{p}, \bar{x}) = \int dp' dx' W(p', x') W_{\text{coh}}(p' - \bar{p}, x' - \bar{x}) ,$$

which is real and positive-definite. On the other hand, the Kirkwood function is complex. All these distributions are expected to reduce to the same phase-space distribution in the $\hbar \rightarrow 0$ limit.

B. Quantum Phase-Space Quark Distributions in the Proton

In this subsection, we generalize the concept of phase-space distributions to relativistic quarks and gluons in the proton. In quantum field theory, the single-particle wave function must be replaced by quantum fields, and hence it is natural to introduce the *Wigner operator*,

$$\hat{\mathcal{W}}_F(\vec{r}, k) = \int d^4\eta e^{ik \cdot \eta} \bar{\Psi}(\vec{r} - \eta/2) \Gamma \Psi(\vec{r} + \eta/2) , \quad (21)$$

where \vec{r} is the quark phase-space position and k the phase-space four-momentum conjugated to the spacetime separation η . Γ is a Dirac matrix defining the types of quark densities because the quarks are spin-1/2 relativistic particles. Depending on the choice of Γ , we can have vector, axial vector, or tensor density.

Since QCD is a gauge theory, the two quark fields at different spacetime points are not automatically gauge-invariant. One can define a gauge-invariant quark field by adding a gauge link to the spacetime infinity along a constant four-vector n^μ ,

$$\Psi(\eta) = \exp \left(-ig \int_0^\infty d\lambda n \cdot A(\lambda n + \eta) \right) \psi(\eta) , \quad (22)$$

where we assume the non-singular gauges in which the gauge potential vanish at the space-time infinity [33, 34, 35, 36, 37]. Clearly, the Wigner operator depends on the choice of n^μ . While theoretically any n^μ is possible, experimentally n^μ is constrained by the probes.

We have extended the Wigner distribution to including the time variable. Therefore, beside the dependence on the 3-momentum, there is also a dependence on the energy. For the bound states in a simple system such as those in a simple harmonic oscillator, the energy dependence is a δ -function at the binding energies. For many-body systems, however, the energy-dependence is more complicated, as it reflects the distribution of the states after one particle is removed from the system.

For non-relativistic systems for which the center-of-mass is well-defined and fixed, one can define the phase-space distributions by taking the expectation value of the above Wigner operators in the $\vec{R} = 0$ state. For the proton for which the recoil effect cannot be neglected, the rest-frame state cannot be uniquely defined, as discussed in Section II. Here we follow Sachs, defining a rest-frame matrix element as that in the Breit frame, averaging over all possible 3-momentum transfers. Therefore, we construct the quantum phase-space quark distribution in the proton as,

$$\begin{aligned} W_\Gamma(\vec{r}, k) &= \frac{1}{2M_N} \int \frac{d^3\vec{q}}{(2\pi)^3} \langle \vec{q}/2 | \hat{\mathcal{W}}_\Gamma(\vec{r}, k) | -\vec{q}/2 \rangle \\ &= \frac{1}{2M_N} \int \frac{d^3\vec{q}}{(2\pi)^3} e^{-i\vec{q}\cdot\vec{r}} \langle \vec{q}/2 | \hat{\mathcal{W}}_\Gamma(0, k) | -\vec{q}/2 \rangle, \end{aligned} \quad (23)$$

where the plane-wave states are normalized relativistically. The most general phase-space distribution depends on *seven* independent variables.

The only way we know how to probe the single-particle distributions is through high-energy processes, in which the light-cone energy $k^- = (k^0 - k^z)/\sqrt{2}$ is difficult to measure, where the z -axis refers to the momentum direction of a probe. Moreover, the leading observables in these processes are associated with the “good” components of the quark (gluon) fields in the sense of light-cone quantization [27], which can be selected by $\Gamma = \gamma^+$, $\gamma^+\gamma_5$, or $\sigma^{+\perp}$ where $\gamma^+ = (\gamma^0 + \gamma^z)/\sqrt{2}$. The direction of the gauge link, n^μ , is then determined by the trajectories of high-energy partons traveling along the light-cone $(1, 0, 0, -1)$ [36, 37]. Therefore, from now on, we restrict ourselves to the reduced Wigner distributions by integrating out k^- ,

$$W_\Gamma(\vec{r}, \vec{k}) = \int \frac{dk^-}{(2\pi)^2} W_\Gamma(\vec{r}, k), \quad (24)$$

with a light-cone gauge link is now implied. Unfortunately, there is no known experiment at present capable of measuring this 6-dimensional distribution which may be called the *master* or *mother* distribution.

Further phase-space reductions lead to measurable quantities. Integrating out the transverse momentum of partons, we obtain a 4-dimensional quantum distribution

$$\begin{aligned} \tilde{f}_\Gamma(\vec{r}, k^+) &= \int \frac{d^2\vec{k}_\perp}{(2\pi)^2} W_\Gamma(\vec{r}, \vec{k}) \\ &= \frac{1}{2M_N} \int \frac{d^3\vec{q}}{(2\pi)^3} e^{-i\vec{q}\cdot\vec{r}} \int \frac{d\eta^-}{2\pi} e^{i\eta^- k^+} \langle \vec{q}/2 | \bar{\Psi}(-\eta^-/2) \Gamma \Psi(\eta^-/2) | -\vec{q}/2 \rangle. \end{aligned} \quad (25)$$

The matrix element under the integrals is what defines the GPDs. More precisely, if one replaces k^+ by Feynman variable xp^+ ($p^+ = E_q/\sqrt{2}$, proton energy $E_q = \sqrt{M^2 + \vec{q}^2/4}$)

and η^- by λ/p^+ , the reduced Wigner distribution becomes the Fourier transformation of the GPD $F_\Gamma(x, \xi, t)$

$$f_\Gamma(\vec{r}, x) = \frac{1}{2M_N} \int \frac{d^3\vec{q}}{(2\pi)^3} e^{-i\vec{q}\cdot\vec{r}} F_\Gamma(x, \xi, t) . \quad (26)$$

In the present context, the relation between kinematic variables are $\xi = q^z/(2E_q)$ and $t = -\vec{q}^2$. Taking $\Gamma = \sqrt{2}\gamma^+$, the corresponding GPD has the expansion [12]

$$\begin{aligned} F_{\gamma^+}(x, \xi, t) &= \int \frac{d\lambda}{2\pi} e^{i\lambda x} \langle \vec{q}/2 | \bar{\psi}(-\lambda n/2) \mathcal{L} \sqrt{2}\gamma^+ \psi(\lambda n/2) | -\vec{q}/2 \rangle \\ &= H(x, \xi, t) \bar{U}(\vec{q}/2) \sqrt{2}\gamma^+ U(-\vec{q}/2) + E(x, \xi, t) \bar{U}(\vec{q}/2) \frac{i\sigma^{+i} q_i}{\sqrt{2}M} U(-\vec{q}/2) , \end{aligned} \quad (27)$$

where \mathcal{L} is the shorthand for the light-cone gauge link.

The phase-space function $f_{\gamma^+}(\vec{r}, x)$ can be used to construct 3D images of the quarks for every selected Feynman momentum x in the rest frame of the proton. These images provide the pictures of the proton seen through the Feynman momentum (or “color” or x) filters. They also may be regarded as the result of a quantum phase-space tomography of the proton. We remind the reader again that the Feynman momentum in the rest-frame sense is a special combination of the off-shell energy and momentum along z , namely $E + k^z$. Integrating over the z coordinate, the GPDs are set to $\xi \sim q^z = 0$, and the resulting two-dimensional density $f_{\gamma^+}(\vec{r}_\perp, x)$ is just the impact-parameter-space distribution [19]. Further integration over \vec{r}_\perp recovers the usual Feynman parton distribution.

The physical content of the above distribution is further revealed by examining its spin structure. Working out the matrix element in Eq. (27),

$$\frac{1}{2M_N} F_{\gamma^+}(x, \xi, t) = [H(x, \xi, t) - \tau E(x, \xi, t)] + i[\vec{s} \times \vec{q}]^z \frac{1}{2M_N} [H(x, \xi, t) + E(x, \xi, t)] , \quad (28)$$

where $\tau = \vec{q}^2/4M_N^2$. The first term is independent of the proton spin, and is considered as the phase-space charge density

$$\rho_+(\vec{r}, x) = \int \frac{d^3\vec{q}}{(2\pi)^3} e^{-i\vec{q}\cdot\vec{r}} [H(x, \xi, t) - \tau E(x, \xi, t)] . \quad (29)$$

The second term depends on the proton spin and can be regarded as the third component of the phase-space vector current

$$j_+^z(\vec{r}, x) = \int \frac{d^3\vec{q}}{(2\pi)^3} e^{-i\vec{q}\cdot\vec{r}} i[\vec{s} \times \vec{q}]^z \frac{1}{2M_N} [H(x, \xi, t) + E(x, \xi, t)] . \quad (30)$$

The E -term generates a convection current due to the orbital angular momentum of massless quarks and vanishes when all quarks are in the s -orbit. The physics in separating f_γ^+ into ρ_+ and j_+^z can be seen from the Dirac matrix γ^+ selected by the high-energy probes, which is a combination of time and space components. Because the current distribution has no spherical symmetry, the quark charge seen in the infinite momentum frame, $\rho_+ + j_+^z$, is deformed in the impact parameter space [38]. This is the kinematic effect of Lorentz boost.

Integrating the phase-space charge distribution $\rho_+(\vec{r}, x)$ over x , one recovers the spherically-symmetric charge density in space. On the other hand, if integrating over x

in $j_+^z(\vec{r}, x)$, one obtains the electric current density. In the latter case, if the integral is weighted with x , one obtains the mechanical momentum density [8].

Finally, when integrating over \vec{r} in the reduced Wigner distributions in Eq. (24), one obtains the transverse-momentum dependent parton distributions.

$$q(x, \vec{k}_\perp) = \frac{M_N}{\sqrt{2}p^+} \int \frac{d^3\vec{r}}{(2\pi)^2} W_+(\vec{r}, \vec{k}) . \quad (31)$$

There is a lot of interesting physics associated with these distributions which has been discussed recently in the literature. For instance, in a transversely polarized proton, the quark momentum distribution has an azimuthal angular dependence [39, 40, 41]. The so-called Siver's function can produce a novel single-spin asymmetry in deep-inelastic scattering. We will not pursue this topic here, except emphasizing that they have the same generating functions as the GPDs.

IV. THREE-DIMENSIONAL IMAGES OF THE QUARKS IN THE PROTON

Once the GPDs are extracted from experimental data or lattice QCD calculations [43, 44, 45, 46], the phase-space distributions can be obtained by straightforward Fourier transformations. Without a first-hand knowledge on the GPDs at present, we may be able to learn some general features of the phase-space distributions from GPD models.

The GPDs have been parametrized directly to satisfy various constraints [15, 17, 47], including 1) the first moments reducing to the measured form factors, 2) the forward limit reproducing the Feynman parton distributions, 3) the x -moments satisfying the polynomiality condition [14], and 4) the positivity conditions [48]. In the first subsection, we introduce a new parametrization without assuming factorized dependence on the t and other variables.

The GPDs were first calculated in a realistic nucleon model—the MIT bag model [49]. They have also been calculated in the chiral-quark soliton model [50, 51]. Recently, there are calculations in the quark models as well [52, 53]. In the second subsection, we will consider the Wigner distributions in the bag model.

A. A GPD Parametrization

A generalized parton distributions depend on three variables, x , ξ , and t . The simplest way to satisfy the polynomiality condition is to relate it to a double distribution [11, 42] and the D -term [50]

$$H(x, \xi, t) = \int_{-1}^1 \frac{dy}{\xi} \Xi(y|x, \xi) F\left(y, \frac{x-y}{\xi}, t\right) + \theta(\xi > |x|) D\left(\frac{x}{\xi}, t\right) , \quad (32)$$

The “step”-function kernel in Eq. (32) has the form

$$\begin{aligned} \Xi(y|x, \xi) = & \theta(x > \xi) \theta\left(\frac{x+\xi}{1+\xi} \geq y \geq \frac{x-\xi}{1-\xi}\right) \\ & + \theta(-\xi > x) \theta\left(\frac{x+\xi}{1-\xi} \geq y \geq \frac{x-\xi}{1+\xi}\right) + \theta(\xi > |x|) \theta\left(\frac{x+\xi}{1+\xi} \geq y \geq \frac{x-\xi}{1-\xi}\right) . \end{aligned}$$

The q -flavor double distribution $F_q = F_q^{\text{val}} + F_q^{\text{sea}}$, including both valence and sea, can be related to the non-forward quark distribution $f_q(y, t)$ through a profile function $\pi(y, z, b)$,

$$F_q^{\text{val}}(y, z, t) = f_q^{\text{val}}(y, t) \theta(y) \pi(|y|, z; b_{\text{val}}), \quad (33)$$

$$F_q^{\text{sea}}(y, z, t) = \left(\bar{f}_q(y, t) \theta(y) - \bar{f}_q(-y, t) \theta(-y) \right) \pi(|y|, z; b_{\text{sea}}), \quad (34)$$

where at $t = 0$ the function $f_q(y, t = 0)$ reduces to the conventional parton distribution functions. The profile function with a single parameter b is assumed to be universal for valence- and sea-quark species, and reads [42]

$$\pi(y, z; b) = \frac{\Gamma(b + 3/2)}{\sqrt{\pi} \Gamma(b + 1)} \frac{[(1 - y)^2 - z^2]^b}{(1 - y)^{2b+1}}. \quad (35)$$

To proceed further, we design a non-factorized ansatz [15, 21, 38] for the functions $f_q(y, t)$ with intertwined t and y dependence. This is opposed to a factorized form of GPDs with completely disentangled dependence of the momentum transfer t and scaling variables (x, ξ) . The latter is currently accepted in almost all evaluations of physical observables [17, 47, 54]. Due to a limited kinematical coverage in the t -channel momentum transfer t in experiments, theoretical estimates confronted to data are currently insensitive to this feature. Our model will be based on the GRV leading order quark distributions [55] with discarded flavor asymmetry of the sea and it reads

$$\begin{aligned} f_u^{\text{val}}(y, t) &= 1.239 y^{-\alpha_v - \alpha'_v (1-y)^{1/2} t} (1 - 1.8\sqrt{y} + 9.5y) (1 - y)^{2.72}, \\ f_d^{\text{val}}(y, t) &= 0.761 y^{-\alpha_v} \left(2y^{-\alpha'_v (1-y)^{1/2} t} - y^{-\beta'_v (1-y)t} \right) (1 - 1.8\sqrt{y} + 9.5y) (1 - y)^{3.62}, \\ \bar{f}_u(y, t) &= \bar{f}_d(y, t) = 0.76 y^{-\alpha_s - \alpha'_s (1-y)^{3/2} t} (1 - 3.6\sqrt{y} + 7.8y) (1 - y)^{9.1}. \end{aligned} \quad (36)$$

These models naturally reduce to the quark form factors with the dipole parametrization of proton and neutron Sachs form factors. The valence d -quark function has a more complicated structure since the corresponding form factor F_1^d has a node at $|t| \approx 4M^2/[2\kappa_n + \kappa_p + 1]$: it is positive below this value and is negative above it. The Regge intercepts and slope parameters are taken as

$$\begin{aligned} \alpha_v &= 0.52, & \alpha'_v &= 1.1 \text{ GeV}^{-2}, & \beta'_v &= 1.0 \text{ GeV}^{-2}, \\ \alpha_s &= 0.85, & \alpha'_s &= 0.3 \text{ GeV}^{-2}. \end{aligned} \quad (37)$$

The valence quarks Regge parameters are numerically close to the ones of ρ -reggeons, while the sea quarks being generated by gluon radiation are analogous to the one of the pomeron. The form factor asymptotics at large t is governed by the large- y behavior of $f(y, t)$. If the latter has the form $f(y, t) \sim y^{-\alpha - \alpha' (1-y)^p t} (1 - y)^N$ then the corresponding form factor is $F(t \rightarrow \infty) \sim |t|^{-(N+1)/(p+1)}$. The perturbative QCD asymptotics for valence quarks requires $p = 1$. We use however $p = 1/2$ for them since this value fits better the form factor at small and moderate t . For $p = 1$ one can get a decent behavior at moderate t with $\alpha'_u = 1.6 \text{ GeV}^2$. We use in our estimates $b_{\text{val}} = b_{\text{sea}} = 1$. The D -term is parametrized as

$$D(z, t) = \left(1 - \frac{t}{m_D^2} \right)^{-3} (1 - z^2) \left(d_0 C_1^{3/2}(z) + \dots \right), \quad (38)$$

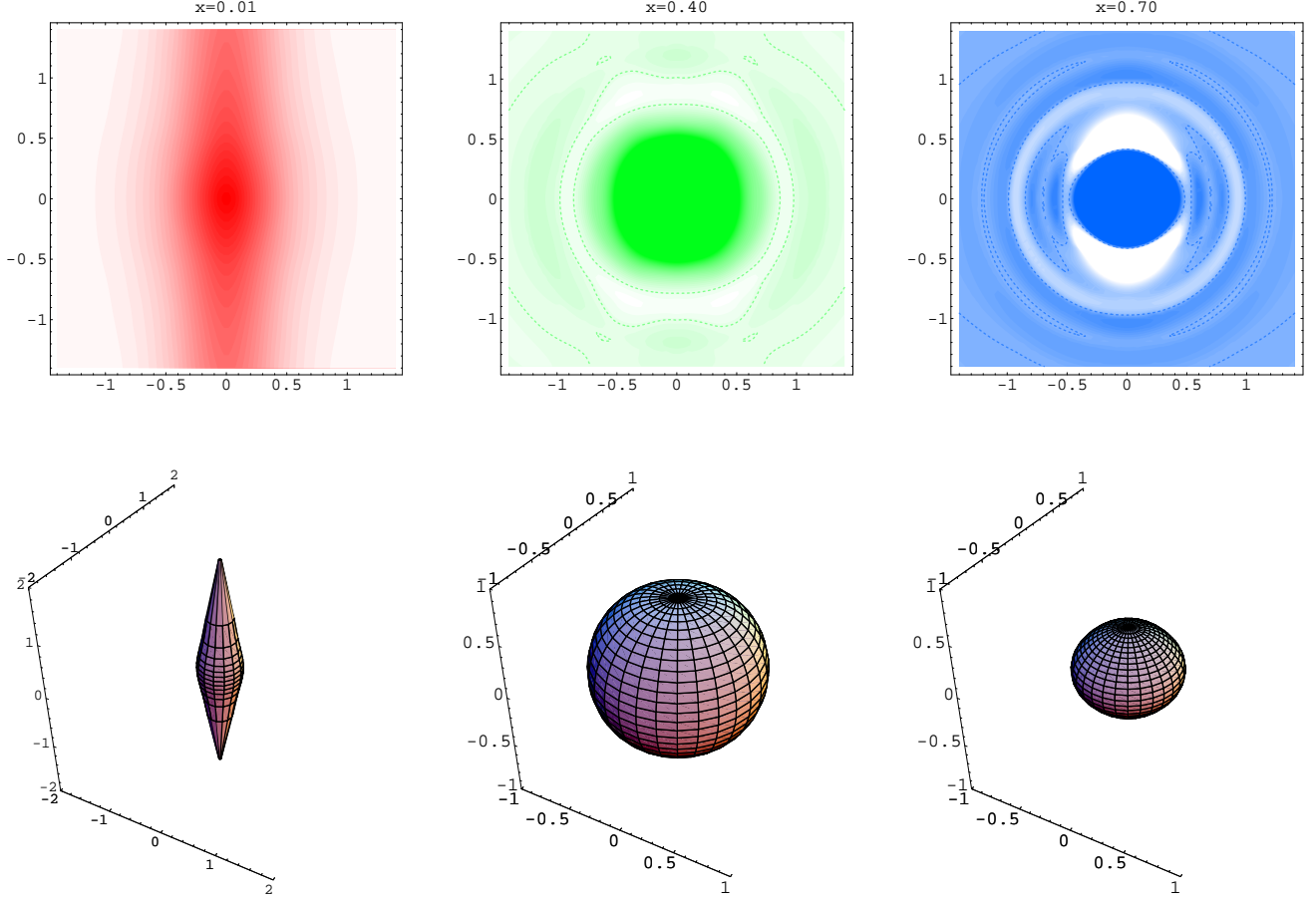


FIG. 1: The u -quark phase-space charge distribution at different values of the Feynman momentum for non-factorizable ansatz of generalized parton distributions (36). The vertical and horizontal axis corresponds to z and $|\vec{r}_\perp|$, respectively, measured in femtometers. The [dashed] contours separate regions of positive [darker areas] and negative [lighter areas] densities. Below each contour plot we presented the shape of three-dimensional isodensity contours $[\rho = \text{const}]$.

with the mass scale $m_D^2 = 0.6 \text{ GeV}^2$ and the parameter d_0 computed within the χQSM [15, 51] and on the lattice [45, 46] with the results

$$d_0^{\chi\text{QSM}} = -4.0 \frac{1}{N_f}, \quad d_0^{\text{latt}} = d_0^u \approx d_0^d \approx -0.5, \quad (39)$$

respectively, where N_f is the number of active flavors. In the lattice case, the effect of disconnected diagrams was not calculated, however they are known to produce a sizable negative contribution [44]. Once the latter are properly taken into account the lattice result might approach the model calculation. For our present estimate we chose an intermediate value $d_0 = -1.0$.

According to the previous section, the phase-space charge distribution $\rho_+(\vec{r}, x)$ is just the Fourier transformation of the above GPDs,

$$\rho_+^q(\vec{r}, x) = \int \frac{d^3\vec{q}}{(2\pi)^3} e^{-i\vec{q}\cdot\vec{r}} H^q(x, \xi, t), \quad (40)$$

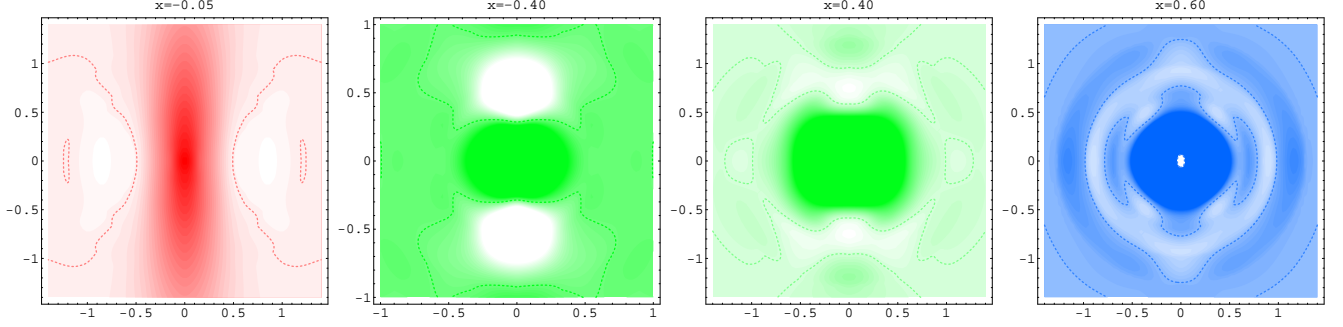


FIG. 2: The phase-space charge distribution for the u -quark at negative Feynman momentum $x = -0.05$ and $x = -0.4$ [two left panels] and d -quark for positive $x = 0.4$ and $x = 0.6$ [two right panels].

where $\xi = q_z/2E_q$, $E_q = \sqrt{M^2 + \vec{q}^2/4}$, and $t = \vec{q}^2$. In the following, we consider the result of the quark densities from the above parametrization.

In Fig. 1 we show the up-quark charge distributions calculated from $H_u(x, \xi, t)$ for various values of $x = \{0.01, 0.4, 0.7\}$. While the intensity of the plots indicates the magnitude of the positive distribution, the lighter areas below the ground-zero contours indicate negative values. The plots show significant change in the distribution on the longitudinal momentum fraction x . The image is rotationally symmetric in the \vec{r}_\perp -plane. At small x , the distribution extends far beyond the nominal nucleon size along the z direction. The physical explanation for this is that the position space uncertainty of the quarks is large when x is small, and therefore the quarks are de-localized along the longitudinal direction. This de-localization reflects a very peculiar part of the nucleon wave function and shows long-range correlations as verified in high-energy scattering. In a nucleus, the parton distributions at small x are strongly modified because of the spatial overlap between the nucleons. On the other hand, at larger x , the momentum along z direction is of order nucleon mass, the quarks are localized to within $1/M_N$. The quantum mechanical nature of the distribution becomes distinct because there are significant changes in the sign at different spatial regions.

It is also interesting to explore the distribution at negative x . We show in Fig. 2 [two left panels] the Wigner densities for the up-quark in the proton for $x: -0.05$ and -0.4 . These plots show significantly-different pattern than those of the positive x . Finally, the two right panels we show the density for the down-quark in the proton. The essential features are quite similar to those of the up-quark densities.

B. The MIT Bag Model

The MIT bag model was invented more than a quarter of a century ago [56]. The model was motivated by the color confinement property of QCD. Massless quarks are confined to a cavity of radius R , and move freely inside. The quark wave function is ultra-relativistic and can be solved from the free Dirac equation with spherical boundary conditions. The bag model has been used to calculate many static properties of the nucleon and has had many notable successes. The model can also be used to describe the excitation spectrum of hadrons [56]. The electromagnetic form factors [57] and parton distributions have also been

calculated for the bag quarks [58].

The bag model has been used to calculate the GPDs in Ref. [49], where the boosted bag wave function has been constructed using a simple prescription. In principle, one can perform a Fourier transformation of the GPDs to calculate the bag-model Wigner distribution.

However, we choose a simpler way to calculate the Wigner distribution because the static bag has a fixed center. In fact, we can calculate directly from the wave function of quarks in the static nucleon just like in non-relativistic quantum mechanics. The rational for this is that assuming the GPDs are known, one can “correct” the relativistic effects associated with the boosted nucleon to obtain a Wigner distribution corresponding to the static structure, just like applying the relativistic corrections to extracting the static charge distributions. The Wigner distributions calculated from a static bag correspond to the ones with some relativistic corrections applied.

As we have discussed in the last section, we define the Wigner distributions by the matrix elements of the Wigner operators $\mathcal{W}_+(\vec{r}, k^+)$ in the hadron states. In general, because of translational invariance, only the off-diagonal matrix elements between nucleon states with finite momentum differences provide the 3D \vec{r} dependence. However, in the static models such as the MIT bag, the quark wave functions are solved in the rest frame of the nucleon which has no translational invariance from start. With them, the Wigner distributions can be calculated as the diagonal matrix elements of the Wigner operator for the model nucleon fixed at the origin of the coordinates. For example,

$$\rho_+(\vec{r}, x) = \frac{1}{2} \int \frac{d\lambda}{2\pi} e^{ix\lambda} \langle \vec{R} = 0 | \bar{\Psi}(\vec{r} - (\lambda/2)n^-) \gamma^+ \Psi(\vec{r} + (\lambda/2)n^-) | \vec{R} = 0 \rangle, \quad (41)$$

where $|\vec{R} = 0\rangle$ represents the bag-model nucleon at $\vec{R} = 0$ and $x = k^+/p^+$ the light-cone momenta fraction of the proton carried by the quark, n a light-light vector with $n^+ = 0, n^- = 1/p^+, n_\perp = 0$.

The quark field has the following expansion in the bag [56]

$$\Psi_\alpha(\vec{r}, t) = \sum_{n>0, \kappa=\pm 1, m} N(n\kappa) \{ b_\alpha(n\kappa m) \psi_{n\kappa j=1/2m}(\vec{r}, t) + d_\alpha^\dagger(n\kappa m) \psi_{-n-\kappa j=1/2m}(\vec{r}, t) \}, \quad (42)$$

where b_α^\dagger and d_α^\dagger are the quark and anti-quark creation operators in the bag, and $N(n\kappa)$ is a normalization factor. The wave function are solved from the Dirac equation with the bag boundary condition. For $j = 1/2$ and $\kappa = -1$, one has

$$\psi_{n,-1, \frac{1}{2}m}(\vec{r}, t) = \frac{1}{\sqrt{4\pi}} \begin{pmatrix} i j_0\left(\frac{\omega_{n,-1}|\vec{r}|}{R_0}\right) \chi_m \\ -\vec{\sigma} \cdot \hat{r} j_1\left(\frac{\omega_{n,-1}|\vec{r}|}{R_0}\right) \chi_m \end{pmatrix} e^{-i\omega_{n,-1}t/R_0}. \quad (43)$$

For the lowest mode, we have $n = 1$, and $\omega_{1,-1} \approx 2.04$. In the above wave function, $\vec{\sigma}$ is the 2×2 Pauli matrix, χ_m is the Pauli spinor, and R_0 is the bag radius. \hat{r} represents the unit vector in the \vec{r} direction, and j_i are sphere Bessel functions.

Substitute the above wave function into Eq. (41), we find the quark phase-space charge density,

$$\begin{aligned} \rho_+^f(\vec{r}, x) = C_f \frac{N^2}{4\pi} \int \frac{d\lambda}{2\pi} e^{i\lambda(x - \frac{\omega}{MR_0})} [j_0(r_1)j_0(r_2) + j_1(r_1)j_1(r_2)\hat{r}_1 \cdot \hat{r}_2 \\ + i(j_0(r_1)j_1(r_2)\hat{r}_2^z - j_0(r_2)j_1(r_1)\hat{r}_1^z)] , \end{aligned} \quad (44)$$

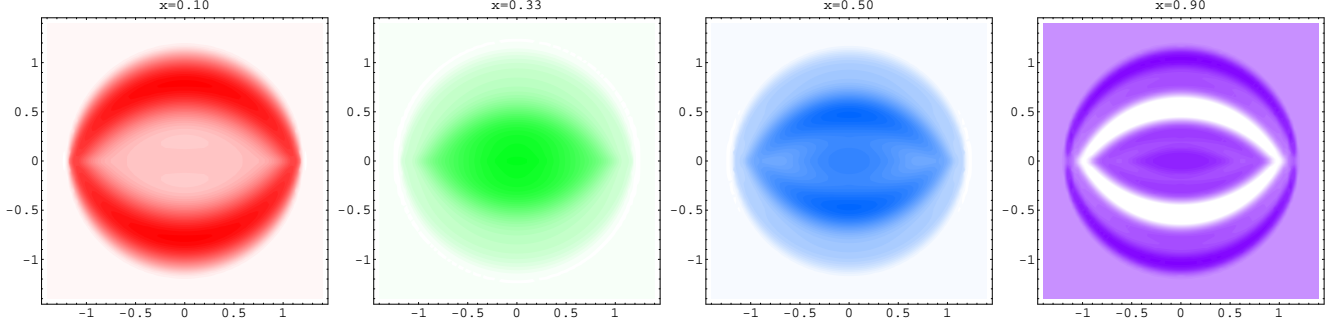


FIG. 3: The phase-space charge density $\rho_+(\vec{r}, x)$ calculated in the bag model for values of Feynman momentum $x = 0.1, 0.33, 0.5, 0.9$.

where C_f is a flavor factor with $C_u = 2$ and $C_d = 1$ for up and down quarks, respectively. The position vectors \vec{r}_1 and \vec{r}_2 are

$$\vec{r}_1 = \vec{r} + \frac{\lambda}{2} \frac{1}{\sqrt{2}p^+} \hat{e}^z, \quad \vec{r}_2 = \vec{r} - \frac{\lambda}{2} \frac{1}{\sqrt{2}p^+} \hat{e}^z. \quad (45)$$

The above distribution satisfies the boundary constraint: Integrating over \vec{r} yields the quark distribution function, while integrating over x gives the charge density of the quarks inside the nucleon.

With $\rho_+(\vec{r}, x)$, one can visualize the quark charge density as the function of x . In Fig. 3, we have shown a sequence of densities at $x = 0.1, 0.33, 0.5$ and 0.9 . As the parton density indicates, the charge density is peaked around $x = 1/3$ where the distribution is roughly spherical-symmetric. This is consistent with the finding that the bag model GPDs have a small ξ dependence. For smaller and larger x , the charge density can be negative. As x increases, the distribution at the center of the bag becomes smaller. As x further increases, the density there becomes negative. Similar phenomena happens as x decreases. Because the bag boundary limits the distance of the spatial correlation, the small- x distribution does not grow significantly as seen in experimental data.

V. SUMMARY AND CONCLUSIONS

In this paper, we have introduced the concept of the quantum phase-space distributions for the quarks and gluons in the nucleon. These distributions contain much more information than conventional observables. In particular, various reductions of the distribution lead to transverse-momentum dependent parton distributions and generalized parton distributions.

Any knowledge on the GPDs can be immediately translated into the correlated coordinate and momentum distributions of partons. In particular, the GPDs can now be used to visualize the phase-space motion of the quarks, and hence allow studying the contribution of the quark orbital angular momentum to the spin of the nucleon.

In light of this, measurements of GPDs and/or direct lattice QCD calculations of them will provide a fantastic window to the quark and gluon dynamics in the proton.

We thank M. Burkardt and T. Cohen for many helpful discussions on the subject of the paper, and M. Diehl for critical comments. We thank the Department of Energy's Institute

for Nuclear Theory at the University of Washington for its hospitality during the program “Generalized parton distributions and hard exclusive processes” and the Department of Energy for the partial support during the completion of this paper. This work was supported by the U. S. Department of Energy via grant DE-FG02-93ER-40762.

-
- [1] E.P. Wigner, Phys. Rev. 40 (1932) 749.
 - [2] N. Balasz, B. Jennings, Phys. Rept. 104 (1984) 347;
M. Hillery, R.F. O’Connell, M.O. Scully, E.P. Wigner, Phys. Rept. 106 (1984) 121;
H.-W. Lee, Phys. Rept. 259 (1995) 147.
 - [3] K. Vogel, H. Risken, Phys. Rev. A 40 (1989) 2847.
 - [4] D.T. Smithey, M. Beck, M.G. Raymer, A. Faridani, Phys. Rev. Lett. 70 (1993) 1244;
G. Breitenbach, S. Schiller, J. Mlynek, Nature 387 (1997) 471.
 - [5] K. Banaszek, C. Radzewicz, K. Wodkiewicz, J.S. Krasinski, Phys. Rev. A 60 (1999) 674.
 - [6] E.J. Ernst, R.G. Sachs, K.C. Wali, Phys. Rev. 119 (1960) 1105;
R.G. Sachs, Phys. Rev. 126 (1962) 2256.
 - [7] R.P. Feynman, *Photon-Hadron Interactions*, Benjamin (New York, 1972).
 - [8] X. Ji, *Viewing the proton through “color” filters*, hep-ph/0304037, to appear in Phys. Rev. Lett. (2003).
 - [9] A.V. Belitsky, *Renormalons in exclusive meson electroproduction*, hep-ph/0307256.
 - [10] See, e.g., J. C. Collins, Acta Phys. Polon. B 34 (2003) 3103 and references therein.
 - [11] D. Müller, D. Robaschik, B. Geyer, F.-M. Dittes, J. Horejsi, Fortschr. Phys. 42 (1994) 101.
 - [12] X. Ji, Phys. Rev. Lett. 78 (1997) 610; Phys. Rev. D 55 (1997) 7114.
 - [13] A.V. Radyushkin, Phys. Rev. D 56 (1997) 5524.
 - [14] X. Ji, J. Phys. G 24 (1998) 1181.
 - [15] K. Goeke, M.V. Polyakov, M. Vanderhaeghen, Prog. Part. Nucl. Phys. 47 (2001) 401.
 - [16] A.V. Radyushkin, *Generalized parton distributions*, in *At the frontier of particle physics*, vol. 2, ed. M. Shifman, World Scientific (Singapore, 2001) p. 1037, hep-ph/0101225.
 - [17] A.V. Belitsky, D. Müller, A. Kirchner, Nucl. Phys. B 629 (2002) 323.
 - [18] D.E. Soper, Phys. Rev. D 15 (1977) 1141.
 - [19] M. Burkardt, Phys. Rev. D 62 (2000) 071503.
 - [20] J.P. Ralston, B. Pire, Phys. Rev. D 66 (2002) 111501.
 - [21] A.V. Belitsky, D. Müller, Nucl. Phys. A 711 (2002) 118.
 - [22] M. Diehl, Eur. Phys. J. C 25 (2002) 223.
 - [23] D. Yennie, M. Ravenhall, M. Levy, Rev. Mod. Phys. 29 (1957) 144.
 - [24] A.L. Licht, A. Pagnamenta, Phys. Rev. D 2 (1970) 1150.
 - [25] X. Ji, Phys. Lett. B 254 (1991) 456;
G. Holzwarth, Z. Phys. A 356 (1996) 339.
 - [26] J. Kelly, Phys. Rev. C 66 (2002) 065203.
 - [27] S.J. Brodsky, H.-C. Pauli, S.S. Pinsky, Phys. Rept. 301 (1998) 299;
M. Burkardt, Adv. Nucl. Phys. 23 (1996) 1.
 - [28] X. Ji, R. McKeown, Phys. Lett. B 236 (1990) 130.
 - [29] A. Dragt, S. Habib, *How Wigner function transforms under symplectic maps*, in *Quantum Aspects of Beam Physics*, ed. P. Chen, World Scientific (Singapore, 1998) p. 651, quant-ph/9806056.

- [30] H.J. Groenewold, *Physica* 12 (1946) 405.
- [31] L. Cohen, *J. Math. Phys.* 7 (1966) 781.
- [32] K. Husimi, *Proc. Phys. Math. Soc. Japan* 22 (1940) 264;
J.G. Kirkwood, *Phys. Rev.* 44 (1933) 31.
- [33] A.V. Efremov, A.V. Radyushkin, *Theor. Math. Phys.* 44 (1981) 774.
- [34] J.M.F. Labastida, G. Sterman, *Nucl. Phys. B* 254 (1985) 425.
- [35] J.C. Collins, D.E. Soper, G. Sterman, *Factorization of hard process in QCD*, in *Perturbative QCD*, ed. A.H. Mueller, World Scientific (Singapore, 1989) p. 1.
- [36] J.C. Collins, *Phys. Lett. B* 536 (2002) 43.
- [37] A.V. Belitsky, X. Ji, F. Yuan, *Nucl. Phys. B* 656 (2003) 165.
- [38] M. Burkardt, *Int. J. Mod. Phys. A* 18 (2003) 173.
- [39] D. Sivers, *Phys. Rev. D* 41 (1990) 83;
D. Boer, P.J. Mulders, *Phys. Rev. D* 57 (1998) 5780.
- [40] S.J. Brodsky, D.S. Hwang, I. Schmidt, *Phys. Lett. B* 530 (2002) 99.
- [41] X. Ji, F. Yuan, *Phys. Lett. B* 543 (2002) 66.
- [42] A.V. Radyushkin, *Phys. Lett. B* 449 (1999) 81.
- [43] N. Mathur, S.J. Dong, K.F. Liu, L. Mankiewicz, N.C. Mukhopadhyay, *Phys. Rev. D* 62 (2000) 114504.
- [44] V. Gadiyak, X. Ji, C. Jung, *Phys. Rev. D* 65 (2002) 094510.
- [45] M. Göckeler, R. Horsley, D. Pleiter, P.E.L. Rakow, A. Schäfer, G. Schierholtz, W. Schroers, *Generalized parton distributions in lattice QCD*, hep-ph/0304249.
- [46] P. Hägler, J.W. Negele, D.R. Renner, W. Schroers, Th. Lippert, K. Schilling, *Moments of nucleon generalized parton distributions in lattice QCD*, hep-lat/0304018.
- [47] A. V. Belitsky, D. Müller, L. Niedermeier, A. Schäfer, *Nucl. Phys. B* 593 (2001) 289.
- [48] P. V. Pobylitsa, *Phys. Rev. D* 66 (2002) 094002.
- [49] X. Ji, W. Melnitchouk, X. Song, *Phys. Rev. D* 56 (1997) 5511.
- [50] M.V. Polyakov, C. Weiss, *Phys. Rev. D* 60 (1999) 114017.
- [51] V.Y. Petrov, P.V. Pobylitsa, M.V. Polyakov, I. Bornig, K. Goeke, C. Weiss, *Phys. Rev. D* 57 (1998) 4325.
- [52] S. Boffi, B. Pasquini, M. Traini, *Nucl. Phys. B* 649 (2003) 243;
P. Schweitzer, S. Boffi, M. Radici, *Phys. Rev. D* 66 (2002) 114004.
- [53] S. Scopetta, V. Vento, *Eur. Phys. J. A* 16 (2003) 527.
- [54] A. Freund, *Detailed QCD analysis of twist-3 effects in DVCS observables*, hep-ph/0306012.
- [55] M. Gluck, E. Reya, A. Vogt, *Eur. Phys. J. C* 5 (1998) 461.
- [56] A. Chodos, R.L. Jaffe, K. Johnson, C.B. Thorn, V. Weisskopf, *Phys. Rev. D* 9 (1974) 3471;
A. Chodos, R. L. Jaffe, K. Johnson, C.B. Thorn, *Phys. Rev. D* 10 (1974) 2599.
- [57] M. Betz, R. Goldflam, *Phys. Rev. D* 28 (1983) 2848;
X. Song, J.S. McCarthy, *Phys. Rev. C* 46 (1992) 1077 (1992).
- [58] R.L. Jaffe, *Phys. Rev. D* 11 (1975) 1953;
A.W. Schreiber, A.I. Signal, A.W. Thomas, *Phys. Rev. D* 44 (1991) 2653.